



1 **Large watershed flood forecasting with high resolution**
2 **distributed hydrological model**

3 Yangbo Chen¹, Ji Li¹, Huanyu Wang¹, Jianming Qin¹, Liming Dong¹

4
5 ¹Department of Water Resources and Environment, Sun Yat-sen University,
6 Guangzhou 510275, China

7
8 *Correspondence to:* Yangbo Chen (eescyb@mail.sysu.edu.cn)

9
10 **Abstract:** Flooding is one of the most devastating natural disasters in the world with
11 huge damages, and flood forecasting is one of the flood mitigation measurements.
12 Watershed hydrological model is the major tool for flood forecasting, although the
13 lumped watershed hydrological model is still the most widely used model, the
14 distributed hydrological model has the potential to improve watershed flood
15 forecasting capability. Distributed hydrological model has been successfully used in
16 small watershed flood forecasting, but there are still challenges for the application in
17 large watershed, one of them is the model's spatial resolution effect. To cope with this
18 challenge, two efforts could be made, one is to improve the model's computation
19 efficiency in large watershed, another is implementing the model on high performance
20 supercomputer. By employing Liuxihe Model, a physically based distributed
21 hydrological model, this study sets up a distributed hydrological model for the flood
22 forecasting of Liujiang River Basin in southern China that is a large watershed.
23 Terrain data including DEM, soil type and land use type are downloaded from the
24 website freely, and the model structure with a high resolution of 200m*200m grid cell
25 is set up. The initial model parameters are derived from the terrain property data, and
26 then optimized by using the PSO algorithm, the model is used to simulate 29 observed
27 flood events. It has been found that by dividing the river channels into virtual channel
28 sections and assuming the cross section shapes as trapezoid, the Liuxihe Model
29 largely increases computation efficiency while keeping good model performance, thus
30 making it applicable in larger watersheds. This study also finds that parameter



31 uncertainty exists for physically deriving model parameters, and parameter
32 optimization could reduce this uncertainty, and is highly recommended. Computation
33 time needed for running a distributed hydrological model increases exponentially at a
34 power of 2, not linearly with the increasing of model spatial resolution, and the
35 200m*200m model resolution is proposed for modeling Liujiang River Basin flood
36 with Liuxihe Model in this study. To keep the model with an acceptable performance,
37 minimum model spatial resolution is needed. The suggested threshold model spatial
38 resolution for modeling Liujiang River Basin flood is 500m*500m grid cell, but the
39 model spatial resolution at 200m*200m grid cell is recommended in this study to keep
40 the model a better performance.

41 **Key words:** watershed flood forecasting, distributed hydrological model, Liuxihe
42 Model, parameter optimization, model spatial resolution

43

44 **1 Introduction**

45 Flooding is one of the most devastating natural disasters in the world, and huge
46 damages has been caused (Krzmm, 1992, Kuniyoshi, 1992, Chen, 1995, EEA, 2010).
47 Flood forecasting is one of the most widely used flood mitigation measurements, and
48 watershed hydrological model is the major tool for flood forecasting. Currently the
49 most popular hydrological model for watershed flood forecasting is still the so-called
50 lumped model (Refsgaard et. al., 1996), which averages the terrain property and
51 precipitation over the watershed, so do the model parameters. Hundreds of lumped
52 models have been proposed and widely used, such as the Sacramento model proposed
53 by Burnash et. al. (1995), the Tank model proposed by Sugawara et. al. (1995), the
54 Xinanjiang model proposed by Zhao (1977), and the ARNO model proposed by
55 Todini (1996), only naming a few among others. It is widely accepted that the
56 precipitation for driving the watershed hydrological processes is usually unevenly
57 distributed over the watershed, particularly for the large watershed, so the lumped
58 model could not easily forecast the watershed flooding of large watersheds.



59 Furthermore, due to the inhomogeneity of terrain property over the watershed, which
60 is true even in very small watershed, so the watershed flood forecasting could not be
61 forecasted accurately if the model parameters are averaged over the watershed. For
62 this reasons, new models are needed to improve the watershed flood forecasting
63 capability, particularly for large watershed flood forecasting.

64

65 Development of distributed hydrological model in the past decades provides the
66 potential to improve watershed flood forecasting capability. One of the most
67 important features of the distributed hydrological model is that it divides watershed
68 terrain into grid cells, which are regarded to have the same meaning of a real
69 watershed, i.e., the grid cells have their own terrain properties and precipitation. The
70 hydrological processes are calculated at both the grid cell scale and the watershed
71 scale, and the parameters used to calculate hydrological processes are also different at
72 different grid cells. This feature makes it could describe the inhomogeneity of both
73 the terrain property and precipitation over watershed. The distributed feature of the
74 distributed hydrological model is a very important feature compared to lumped model,
75 which makes it could better simulate the watershed hydrological processes at all scale,
76 small or large. The inhomogeneity of precipitation over watershed could also be well
77 described in the model, this is very helpful in modeling large watershed hydrological
78 processes, particularly in the tropical and sub-tropical regions where the flooding is
79 driven by heavy storm. For this reason, distributed hydrological model is usually
80 regarded to have the potential to better simulate or forecast the watershed flood
81 (Ambrose et. al., 1996, Chen et. al., 2016). Employing distributed hydrological
82 model for watershed food forecasting has been a new trend(Vieux et. al., 2004, Chen
83 et. al., 2012, Cđine Catto ĩn et. al., 2016, Witold et. al., 2016, Kauffeldt et. al., 2016).

84

85 The blueprint of distributed hydrological model is regarded to be proposed by Freeze
86 and Harlan (1969), the first distributed hydrological model was the SHE model
87 proposed by Abbott et. al. (1986a, 1986b). Distributed hydrological model requires



88 different terrain property data for every grid cells to set up the model structure, so it is
89 data driven model. In the early stage of distributed hydrological modeling, this posted
90 great challenge for distributed hydrological model's application as the data was not
91 widely available and inexpensively accessible. With the development of remote
92 sensing sensors and techniques, terrain data covering global range with high
93 resolution has got readily available and could be acquired inexpensively. For example,
94 the DEM at 30m grid cell resolution with global coverage could be freely downloaded
95 (Falorni et al., 2005, Sharma et. al., 2014), which largely pushes forward the
96 development and application of the distributed hydrological models. After that, many
97 distributed hydrological models have been proposed, such as the WATERFLOOD
98 model (Kouwen, 1988), THALES model (Grayson et al., 1992), VIC model (Liang et.
99 al., 1994), DHSVM model (Wigmosta et. al., 1994), CASC2D model (Julien et. al.,
100 1995), WetSpa model (Wang et. al., 1997), GBHM model (Yang et. al., 1997), WEP-L
101 model (Jia et. al., 2001), Vflo model (Vieux et. al., 2002), tRIBS model(Vivoni et. al.,
102 2004), WEHY model (Kavvas et al., 2004), Liuxihe model (Chen et. al., 2011, 2016),
103 and more.

104

105 Distributed hydrological model derives model parameters physically from the terrain
106 property data, and is regarded not need to calibrate model parameter, so it could be
107 used in data poor or ungauged basins. This feature of distributed hydrological model
108 made it applied widely in evaluating the impacts of climate changes and urbanization
109 on hydrology(Li et. al., 2009, Seth et. al., 2001, Ott, et. al., 2004, Vanrheenen et. al.,
110 2005, Olivera et. al., 2007). But it also was found that this feature caused parameter
111 uncertainty due to the lack of experiences and references in physically deriving model
112 parameters from the terrain property, so could not be used in fields that require high
113 flood simulated accuracy, including watershed flood forecasting. It was realized that
114 parameter optimization for distributed hydrological model is also needed to improve
115 the model's performance, and a few methods for optimizing parameters of distributed
116 hydrological model have been proposed. For example, Vieux et. al. (2003) tried a



117 so-called scalar method to adjust the model parameters, and the model performance is
118 found to be improved largely. Madsen et. al. (2003) proposed an automatic
119 multi-objective parameter optimization method with SCE algorithm for SHE model,
120 which improved the model performance also. Shafii et. al. (2009) proposed a
121 multi-objective genetic algorithm for optimizing parameters of WetSpa model, the
122 improved model result is regarded to be reasonable. Xu et. al. (2012) proposed an
123 automated parameter optimization method with SCE-UA algorithm for Liuxihe Model,
124 which improved the model performance in a small watershed flood forecasting. Chen
125 et. al. (2016) proposed an automated parameter optimization method based on PSO
126 algorithm for Liuxihe Model watershed flood forecasting, and tested in two watershed,
127 one is small, one is large. The results suggested that distributed hydrological model
128 should optimize model parameters even if there is only little available hydrological
129 data, while the derived model parameters physically from the terrain property could
130 serve as an initial parameters. The above progresses in distributed hydrological
131 model's parameter optimization has matured, and will largely improve the
132 performance of distributed hydrological model, thus pushing forward the application
133 of distributed hydrological model in real-time watershed flood forecasting.

134

135 Spatial resolution is a key factor in distributed hydrological modeling. Theoretically if
136 the spatial resolution of a distributed hydrological model is higher, i.e., the grid cell
137 size is smaller, the terrain property could be described finer, and the hydrological
138 processes could be better simulated or forecasted, so the model spatial resolution
139 should be as high as possible. But on the other hand, higher model spatial resolution
140 requires higher resolution terrain property data for model setting up which may not be
141 available in some watersheds. But the most important is that distributed hydrological
142 model uses complex equations with physical meanings to calculate the hydrological
143 processes, so it needs much more computation resources than that of lumped model,
144 and the required computation resources increases exponentially with the increasing of
145 the model spatial resolution. So in modeling flood processes of a large watershed, the



146 computation time needed for running the distributed hydrological model will be huge
147 if the model spatial resolution is kept high, which may make the model application
148 impractical due to high running cost. So if distributed hydrological model is needed to
149 be applied in large watershed, a coarser resolution is the only choose, and the model's
150 capability will be impacted with less satisfactory results. This is also called the scaling
151 effect of distributed hydrological modeling. For this reason, current application for
152 watershed flood forecasting either limited to small watershed with higher resolution
153 or coarser resolution in large watershed, i.e., a trade-off between the model
154 performance and running cost.

155

156 Nowadays forecasting large watershed flooding has been in great demands as it
157 impacts peoples and their properties at large range, but due to the scale effect, current
158 distributed hydrological models employed for large watershed are at coarser
159 resolution, which lowers its capability for flood forecasting and warning. For example,
160 past application of distributed hydrological model for large watershed flood forecating
161 are at the resolution coarser than 1km grid cell (Lohmann et. al., 1998, Vieux et. al.,
162 2004, Stisen et. al., 2008, Rwetabula et. al., 2007), the models employed in the
163 pan-European Flood Awareness System (EFAS; Bartholmes et. al., 2009, Thielen et.
164 al., 2009, 2010, Sood et. al., 2015, Kauffeldt et. al., 2016) are at 1-10km grid cell,
165 which makes the result only applicaple for flood warning.

166

167 Challenge for distributed hydrological model application in large watershed flood
168 forecasting is its need for huge computation resources, to cope with this challenge,
169 two efforts could be made. One is to improve the computation efficiency of the
170 distributed hydrological modeling in large watershed, another is implementing the
171 model on high performance supercomputer so in the cases that the users are willing to
172 pay a high computation cost, the flood forecasting of large watershed with high
173 resolution could be done. In this study, the Liuxihe Model (Chen et. al., 2011, 2016), a
174 physically based distributed hydrological model proposed for watershed flood



175 forecasting, has been tried for flood forecasting of a large watershed in southern
176 China to validate the feasibility of distributed hydrological model's application for
177 large watershed flood forecasting.

178 **2 Studied river basin and data**

179 **2.1 Liujiang River Basin**

180 The river basin studied in this paper is the Liujiang River Basin(here after referred to
181 as LRB) in southern China, which is the first order tributary of the Pearl River. LRB
182 originates from Village Lang in Guizhou Province, and drains through Guizhou
183 Province, Guangxi Zhuang Autonomous Region and Hunan Province with 72% of its
184 drainage area in Guangxi Zhuang Autonomous Region. The length of its main channel
185 is 1121 km, the total drainage area is 58270 km² that marks it a large river basin in
186 China. Fig. 1 is a sketch map of LRB.

187 Fig. 1 sketch map of Liujiang River Basin(LRB)

188 LRB is a mountainous watershed in southern China. There are high mountains in the
189 north and northwest of the watershed with high elevation, while in its south and
190 southeast area, the elevation is low. This topography helps forming severe flooding in
191 the middle and downstream. The basin is in the sub-tropical monsoon climate zone
192 with an average annual precipitation of 1800 mm, and the precipitation distribution is
193 highly uneven both at spatial and temporal with 80% of its annual precipitation occurs
194 in the summer. LRB is in the center of storm zone of Zhuang Autonomous Region,
195 heavy storm was very frequent in the past. There are 59 disastrous flooding in the past
196 400 years with recording since 1488, which makes LRB the tributary with most
197 serious flooding among all the first order tributaries of the Pearl River. In the
198 watershed, there is no significant flood mitigation project to store flood runoff, so
199 flood forecasting is one of the most effective ways for the flood management.

200 **2.2 Hydrological data**

201 There are 66 rain gauges installed in the watershed. In this study, hydrological data of
202 30 flood events has been collected, including the precipitation of the rain gauges and



203 the river discharge of Liuzhou river gauge that locates in the downstream of the
204 watershed and closes to the outlet as shown in Fig. 1 with a hourly step, brief
205 information of these flood events is listed in Table 1.

206 Table1 Brief information of flood events with data collected in LRB

207 **2.3 Terrain property data**

208 Terrain property data includes DEM, land use/cover map and soil map, which are
209 used for setting up the distributed hydrological model for flood forecasting. In this
210 study, the DEM was downloaded from the SRTM database (Falorni et al., 2005,
211 Sharma et. al., 2014), the land use type was downloaded from the USGS land use type
212 database (Loveland et. al., 1991, Loveland et. al., 2000), and the soil type was
213 downloaded from FAO soil type database (<http://www.isric.org>). The downloaded
214 DEM has a spatial resolution of 90m*90m, considering LRB is large, the running load
215 for the model with a resolution of 90m*90m may be too heavy to run in this study, so
216 the DEM is rescaled to the resolutions of 200m*200m, as shown in Fig. 2(a). The
217 downloaded land use and soil type were at 1000m*1000m resolution, so there are
218 rescaled to the same resolution of DEM, as shown in Fig. 2(b) and Fig. 2 (c)
219 respectively.

220 Fig. 2 Terrain properties of LRB

221 The highest elevation and the lowest elevation of LRB are 2124 m and 42 m
222 respectively. There are 9 land use types, including evergreen needle leaved forest,
223 evergreen broadleaved forest, shrubbery, mountain and alpine meadow, slope
224 grassland, urban area, river, lakes and cultivated land, accounting for 18.1%, 31.0%,
225 32.5%, 0.1%, 13.7%, 0.1%, 0.2%, 0.3% and 4% of the total drainage area respectively.
226 Forestry, including evergreen needle leaved forest and evergreen broadleaved forest is
227 the major land use type with a percentage of 49.1%, shrubbery occupies a big portion
228 of the watershed also with a percentage of 32.5%, slope grassland also has a
229 significant portion with a percentage of 13.7%, other land use types are very less and
230 are not significant, this means LRB is well vegetated.



231

232 There are 11 soil types, including Humicacrisol, Haplic and high activitive acrisol,
233 Ferralic cambisol, Haplicluvisols, Dystric cambisol, Calcaric regosol, Dystric regosol,
234 Haplic and weak active acrisol, Artificial accumulated soil, Eutricregosols and Black
235 limestone soil, Dystric rankers, accounting for 0.8%, 1.5%, 5%, 3.5%, 2.8%, 45.5%,
236 2.9%, 18%, 1.5%, 3.5% and 15% of the total drainage area respectively. Calcaric
237 regosol is the major soil type which occupies 45.5% of the watershed area, almost half
238 of the drainage area, which is mainly in the east side of the watershed. Haplic and
239 weak active acrisol is another major soil type with an area percentage of 18% and is
240 located in the west side of the watershed. Dystric rankers is also a major soil type with
241 an area percentages of 15% which located in the north side of the watershed. Other
242 soil types are not significant with area percentages below 5% respectively and scatted
243 within the watershed.

244 **3 Liuxihe Model for LRB flood forecasting**

245 **3.1 Introduction of Liuxihe Model**

246 Liuxihe Model is a physically based distributed hydrological model proposed mainly
247 for watershed flood forecasting (Chen, 2009, Chen et. al., 2011, 2016). Like other
248 distributed hydrological models, Liuxihe Model divides the watershed into grid cell
249 based on the DEM of the studied watershed. To keep a reasonable model performance,
250 in the past experiences of Liuxihe Model research and application, the model
251 resolution is limited to 90m*90m or 100m*100m, but only used in small watersheds
252 (Chen, 2009, Chen et. al., 2011, 2013, 2016, Liao et. al., 2012 a, b, Xu et. al., 2012 a,
253 b). Precipitation, evaporation and runoff production are calculated at cell scale, runoff
254 routes first on cell, then alone the cell to river channel, and finally to the watershed
255 outlet. As Liuxihe model is mainly used in the sub-tropical regions, so the runoff
256 production is calculated based on the saturation-excess mechanism. The runoff
257 routing is classified as hill slope routing, river channel routing, subsurface routing and
258 underground routing. The hill slope routing is regarded as the one-dimensional
259 unsteady flow, and the kinematical wave approximation is employed to do the routing.



260 The river channel routing is also regarded as the one-dimensional unsteady flow, but
261 the diffusive wave approximation is employed to do the routing. The above methods
262 are widely used in the dominated distributed hydrological models.

263

264 What makes Liuxihe Model different is that the river channel cross section shape is
265 assumed to be trapezoid. With this assumption, the river channel size could be
266 represented with 3 indices, including the bottom width, side slope and bottom slope.
267 One of the advantages with this assumption is that the river channel cross section size
268 could be estimated with remotely sensed data, so Liuxihe Model could do river
269 channel runoff routing real physically, thus making Liuxihe Model a fully distributed
270 hydrological model. As there are too many river channel cross sections, and many of
271 them are in the upstream of the watershed where it is not easily accessed, so in real
272 hydrological modeling, directly measuring the river channel cross section sizes are
273 impractical. For this reason, most of the distributed hydrological model could not be
274 applied in real applications, or simply route the runoff with lumped methods which
275 makes the model not a fully distributed hydrological model, thus lowering the model's
276 capability in simulating or forecasting the watershed flood processes. Another
277 advantage of this assumption is that it also simplifies the runoff routing, thus
278 improves the model's computation efficiency. For this reason, even Liuxihe Model
279 has a very high resolution, it still could be used in real-time flood forecasting. This
280 feature of Liuxihe Model in estimating river channel cross section sizes makes it has
281 the potential to be used in large watershed flood forecasting.

282

283 Like other distributed hydrological model, when used in ungauged or data poor
284 watershed flood forecasting, Liuxihe Model derives model parameters physically
285 from the terrain property data, but automatic parameter optimization methods have
286 been tried, and two methods, including the SCE-UA algorithm (Xu et. al, 2012) and
287 PSO algorithm (Chen et. al., 2016) have been successfully used for Liuxihe Model's
288 parameter optimization. Study results also suggested that the parameter uncertainty is



289 high for the physically derived model parameters, and if there is a few observed
290 hydrological processes data, model parameter optimization is recommended that
291 could improves the model performance largely (Chen et. al., 2016). But as automatic
292 parameter optimization needs thousands model runs, that makes it difficult to be used
293 widely due to huge computing source requirement, which also make it taking long
294 time in setting up the model. For this reason, a public computer cloud was set up for
295 optimizing the parameters of Liuxihe Model which employs parallel computation
296 techniques and was implemented on a supercomputer system(Chen et. al., 2013). With
297 this development, Liuxihe Model could easily optimize its model parameters.

298

299 Above advancements of Liuxihe Model in estimating river channel cross section sizes
300 with remotely sensed data, automatic parameters optimization and supercomputing
301 makes it has the potential to be used in large watershed flood forecasting, so in this
302 study, the Liuxihe model is employed to study the LRB's flood forecasting.

303 **3.2 Liuxihe Model set up**

304 Considering LRB is large, so the DEM with 200m×200m resolution is adopted to set
305 up the model structure, not at the original 90m×90m resolution. The whole watershed
306 is first divided into 1469900 cells by the DEM horizontally, which were further
307 categorized into hill slope cells and river cells. By using Strahler method (Strahler,
308 1957), the river channel is divided into 3 order system as shown in Fig. 3, which
309 divides the whole cells into 1463204 hill slope cells and 6696 river cells.

310 Fig. 3 Liuxihe Model structure set up for LRB (200m×200m resolution)

311 To estimate the river channel sizes, 178 virtual nodes were set on the river channel
312 system, and 225 virtual channel sections were formed as shown in Figure 3. As in
313 Liuxihe Model, the shape of the virtual channel sections is assumed to be trapezoid,
314 so the cross section size is represented by three indices, including bottom width, side
315 slope and bottom slope. As proposed in Liuxihe Model, the bottom width is estimated
316 based on the satellite remote sensing imageries. For the side slope, it is a low sensitive



317 data, so it could be estimated based on local experiences. For the bottom slope, it is
318 calculated with the DEM alone the virtual channel section. As there are too many data
319 for the virtual cross section sizes, so it is not listed in this paper.

320 **3.3 Parameter optimization**

321 In Liuxihe Model, an initial parameter set will be derived first based on the terrain
322 properties, including the DEM, soil type and land use/cover type, then the parameters
323 will be optimized. In this study, for the insensitive parameter of the land use/cover
324 related parameters, which is the evaporation coefficient, the initial value is set to be
325 0.7 for all cells based on the experiences. The initial value of roughness, i.e., the
326 Manning's coefficient, which is the sensitive parameter of the land use/cover related
327 parameters, is derived from the land use/cover type based on references (Chen et.al.,
328 1995, Zhang et.al., 2006, 2007, Shen et.al., 2007, Guo et.al., 2010, Li et.al., 2013,
329 Zhang et.al., 2015), and listed in Table 2.

330 Table 2 The initial values of land use/cover related parameters

331 For the soil related parameters, including the water content at saturation condition, the
332 water content at field condition, the water content at wilting condition, hydraulic
333 conductivity at saturation condition, soil thickness and soil porosity characteristics
334 coefficient b . Based on past modeling experiences and references (Zaradny, 1993,
335 Anderson et al., 1996), a value of 2.5 is set to b for all soil type, and the water content
336 at wilting condition is set to be 30% of the water content at saturation condition. The
337 soil thickness is estimated based on local experiences and listed in Table 3 for all soil
338 types. The initial values of the water content at saturation condition, the water content
339 at field condition and hydraulic conductivity at saturation condition are estimated by
340 using the Soil Water Characteristics Hydraulic Properties Calculator (Arya et al., 1981)
341 based on soil texture, organic matter, gravel content, salinity and compaction. The
342 estimated initial values of soil-related parameters are listed in Table 3.

343 Table 3 The initial values of soil related parameters

344 In Liuxihe Model, Particle Swarm Optimization(PSO) algorithm (Chen et. al., 2016)



345 and SCE-UA algorithm (Xu et. al., 2012) were employed to optimize the initial model
346 parameters. In this study, PSO algorithm is employed to optimize the initial model
347 parameters as PSO algorithm has been integrated into the Liuxihe Model Cloud (Chen
348 et. al., 2013). The number of particles of PSO algorithm is set to 20, while the value
349 range of inertia weight ω is set to 0.1 to 0.9, the value range of acceleration
350 coefficients C1 is set to 1.25 to 2.75, and C2 to 0.5 to 2.5, and the maximum iteration
351 is set to 50. Flood event of 20080609 is selected to optimize the parameters of Liuxihe
352 model, and Fig. 4 shows the result of the parameter optimization. Among them, Fig.
353 4(a) is the parameters evolving process, Fig. 4(b) is the changing curve of objective
354 function which is set to minimize the peak flow error, Fig.4(c) is the simulated
355 hydrograph of flood event 20080609 with the optimized parameters.

356 Fig. 4 Parameter optimization results of Liuxihe Model for LRB with PSO algorithm
357 From the results in Fig. 4, it could be found that after 14 evolutions, the parameters
358 optimization process converges to its optimal values, and the optimal parameters are
359 achieved, the simulated hydrological process of flood event that is used for parameter
360 optimization is quite good fitting the observed hydrological process, it could be said
361 that the parameter has a good optimization effect.

362
363 As mentioned above, the automatic parameter optimization of the distributed
364 hydrological model is very time consuming. In this study, even supercomputer is
365 employed with parallel computation techniques, the time used for this parameter
366 optimization is overwhelming, the total time used for achieving the above optimal
367 parameters of Liuxihe model for LRB flood forecasting is 220 hours, more than 9
368 days. Considering several runs are usually needed before achieving the final results,
369 so the parameter optimization procedure may take a few months, this run time is
370 really a good investment, but the validation results proves this is worth.

371 **3.4 Model validation**

372 The other 29 flood events were simulated by using the Liuxihe model with the above



373 optimized parameters, and the simulated hydrographs of 8 flood events are shown in
374 Fig. 5, the simulated hydrographs of 8 flood events with initial parameters are also
375 shown in Fig. 5.

376 Fig. 5 Simulated flood events by Liuxihe Model with optimized parameters

377 From the result of Fig. 5, it has been found that the simulated flood processes fits the
378 observation reasonable well, particularly the simulated peak flow is quite good, and
379 the simulated hydrological processes with optimized model parameter improved the
380 simulated hydrological processes largely. To further analyze the effect of parameter
381 optimization on model performance improvement, five evaluation indices of the
382 simulated flood events, including the Nash–Sutcliffe coefficient, the correlation
383 coefficient, the process relative error, the peak flow error and water balance
384 coefficient are calculated from the simulated results. Table 4 listed the 5 indices for
385 both the simulated results with the initial parameters and the optimized parameters.

386 Table 4 Evaluation indices of the simulated flood events

387 From Table 4, it could be seen that the five evaluation indices are quite good for the
388 simulated hydrological processes with the optimized model parameters. The average
389 peak flow error is 5% with 14% the maximum. The average Nash–Sutcliffe
390 coefficient, correlation coefficient, process relative error and water balance coefficient
391 are 0.82, 0.83, 0.22 and 0.87 respectively, that are also quite good for large river basin
392 flood simulation. Five evaluation indices of the simulated hydrological processes with
393 the optimized model parameters are also good improvements to those simulated with
394 the initial parameters, those are 0.64, 0.62, 0.37, 0.29 and 0.78. There are excellent
395 improving in all five indices, with the average increases of 0.18, 0.21 and 0.09 of the
396 average Nash–Sutcliffe coefficient, correlation coefficient and water balance
397 coefficient respectively, and the average decreases of the peak flow error and process
398 relative error are 24% and 15% respectively. So it could be concluded that the Liuxihe
399 Model set up in LRB with optimized parameters are reasonable and could be used for
400 flood forecasting of LRB. This also implies that parameter optimization of distributed



401 hydrological model could improve model performances, and it should be done when it
402 is possible.

403 **5 Results and discussions**

404 **5.1 Computation time vs model resolution**

405 To evaluate the spatial resolution scaling effect of distributed hydrological modeling
406 in LRB, the DEM with 90m*90m resolution is rescaled to the resolutions of
407 500m*500m and 1000m*1000m respectively, the land use and soil type at
408 1000m*1000m resolution are also rescaled to the same resolutions of the DEM used.
409 Liuxihe models for LRB flood forecasting at 500m*500m and 1000m*1000m
410 resolution are set up with the above methods, and the model structures are shown in
411 Fig. 6.

412 Fig. 6 Liuxihe Model structure set up for LRB with different resolution

413 With different spatial resolution, the numbers of grid cells, hill slope cells and river
414 cells are different, but the river channel order are all set to 3, the numbers of virtual
415 channel nodes for 500m*500m and 1000m*1000m resolution models are 68 and 33
416 respectively, numbers of grid cells, hill slope cells and river cells with different model
417 resolution are listed in Table 5. , the sizes of every virtual cross sections are measured
418 with the above method.

419 Table 5 Grid cell numbers with different model spatial resolution

420 From Table 7, it could be seen, number of grid cells of the model with 200m*200m
421 resolution is 6.25 times of that with 500m*500m resolution, and 25 times of that with
422 1000m*1000m resolution, it increases at an approximate exponential of power 2, not
423 linearly with the model resolution.

424

425 Parameters of the models with 500m*500m and 1000m*1000m resolution are
426 optimized with PSO algorithm by using the same flood event data, and listed in Table
427 6. From the results it could be seen that some parameters are significantly different



428 with resolution variation, but some changes little, this implies that the model
429 parameters are resolution-dependent.

430 Table 6 Optimized parameters with different model spatial resolution

431 Computation times required for parameter optimization are quite different. For the
432 model with 200m*200m resolution, the time for parameter optimization is 220 hours,
433 while that for models with 500m*500m and 1000m*1000m resolution are 55 and 12
434 hours respectively. The times needed for parameter optimization of the model at
435 200m*200m resolution is 4 times of that for 500m*500m resolution model and 18.3
436 times of that for 1000m*1000m resolution model respectively. Considering the time
437 needed for model run, the 200m*200m model resolution is regarded as appropriate for
438 LRB.

439 **5.2 Model performance vs model resolution**

440 The other 29 flood events are also simulated with the models at 500m*500m
441 resolution and 1000m*1000m resolution. Simulated hydrograph of 5 flood events,
442 including 2 big, 2 medium and one small ones are shown in Fig. 7.

443 Fig. 7 Simulated results with different model resolutions

444 From the results it could be seen that the simulated hydrological processes with 3
445 different spatial resolutions are quite different. The result simulated with
446 1000m*1000m resolution is not so good, although the flood shapes are simulated well,
447 but the peak flow are much lower than that of the observation, so the result is not
448 acceptable, and could not be recommended. The result simulated with 500m*500m
449 resolution model is a big improvement to that simulated with 1000m*1000m
450 resolution model, the flood shapes are more similar to the observation, and the peak
451 flow is also get closer to the observation, and could be recommended for flood
452 forecasting if the spatial resolution could not be much finer. The result simulated with
453 200m*200m resolution model is a further improvement to that simulated with
454 500m*500m resolution model, the flood shapes fits the observation much better, and
455 the peak flows are also much closer to the observation also, it is the good simulation



456 results and could be recommended for flood forecasting of LRB. The results are good
457 enough that there is no need to further explore the finer model resolution.

458 **6 Conclusions**

459 By employing Liuxihe Model, a physically based distributed hydrological model, this
460 study sets up a distributed hydrological model for the flood forecasting of Liujiang
461 River Basin in southern China that could be regarded as a large watershed. Terrain
462 data including DEM, soil type and land use type are downloaded from the website
463 freely, and the model structure with a high resolution of 200m*200m grid cell is set
464 up, which divides the whole watershed into 1469900 grid cells that is further divided
465 into 1463204 hill slope cells and 6696 river cells. The initial model parameters are
466 derived from the terrain property data, and then optimized by using the PSO algorithm
467 with one observed flood event, which improves the model performance largely. 29
468 observed flood events are simulated by using the model with optimized parameters,
469 the results are analyzed, and the model scaling effects are studied. Based on these
470 studies, following conclusions are suggested.

471

472 1. In Liuxihe Model, the river channels are divided into virtual channel sections, and
473 the cross section shapes are assumed to be trapezoid and the size is the same within
474 the virtual channel section. The size of the virtual channel section is simplified to
475 three indices, including bottom width, side slope and bottom slope, those are
476 estimated by using remote sensing imageries. This method not only makes the
477 distributed model application practical, but also simplifies the river channel routing
478 method. This significantly increases the model computation efficiency, and makes it
479 could be used in larger watersheds. Results in this study shows the model setting up
480 with this method has a reasonable performance, i.e., this simplification has not
481 sacrificed the model's flood simulation accuracy significantly, so this simplification
482 could be used in large watershed distributed hydrological modelling, including
483 Liuxihe model and other models.

484



485 2. Uncertainty exists for physically derived model parameters. Parameter optimization
486 could reduce parameter uncertainty, and is highly recommended to do so when there
487 is some observed hydrological data. In this study, the simulated hydrograph with
488 optimized model parameters is more fitting the observed hydrograph in shape than
489 that simulated with initial model parameters, the 5 evaluation indices are improved
490 also. The average increases of Nash–Sutcliffe coefficient, correlation coefficient and
491 water balance coefficient are 0.18, 0.21 and 0.09 respectively, the average decreases
492 of the peak flow error and process relative error are 24% and 15% respectively, this
493 implies that the model performance is improved significantly with parameter
494 optimization.

495

496 3. Computation time needed for running a distributed hydrological model increases
497 exponentially at an approximate power of 2, not linearly with the increasing of model
498 spatial resolution. In this study, the computation time required for parameter
499 optimization for the model with 200m*200m resolution is 220 hours, that is 4 times of
500 that of the model at 500m*500m and 18.3 times of that of the model at 1000m*1000m
501 resolution respectively. Based on the Liuxihe Model cloud system implemented on the
502 high performance supercomputer, the 200m*200m model resolution is the highest
503 resolution that could be fulfilled in modeling Liujiang River Basin flooding with
504 Liuxihe Model considering the computation cost. This also means that if the user
505 could pay high computation cost, then larger watershed could also be modelled with
506 Liuxihe Model by implemented the Liuxihe Model cloud system on a much more
507 advanced high performance supercomputer, this could be easily done nowadays if the
508 user thinks this investment is a worth doing.

509

510 4. In forecasting watershed flood by using distributed hydrological model, minimum
511 model spatial resolution needs to be maintained to keeping the model an acceptable
512 performance. Usually if the model spatial resolution increases, i.e., the grid cell gets
513 smaller, the model performance is better, but this will increase the run time



514 significantly, so there is a threshold model spatial resolution to keep the model
515 performance reasonable while keep the model run at the least time. In this study, the
516 threshold model spatial resolution is at 500m*500m grid cell, but the resolution at
517 200m*200m grid cell is recommended by trading-off between the computation cost
518 and the model performance. This conclusion may be different in different watersheds
519 for Liuxihe Model, or even different in the same watershed for different models.

520

521 5. Terrain data downloaded freely from the website derived the river channel system
522 that is very similar to the natural river channel system after it is rescaled from its
523 original spatial resolution of 90m*90m to 200m*200m, 500m*500m and
524 1000m*1000m, but the higher resolution DEM describes the river channel more in
525 details. This means that the freely downloaded DEM could be used to set up the
526 Liuxihe Model for Liujiang River Basin flood forecasting.

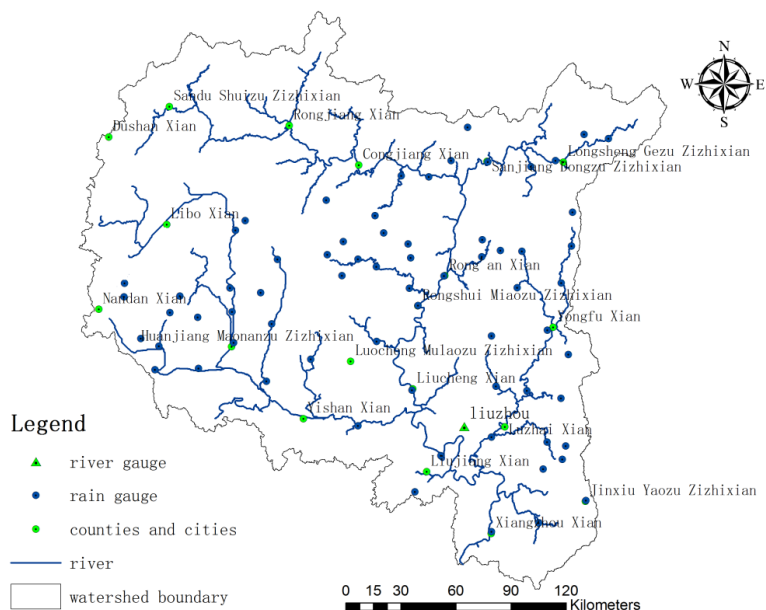
527

528 **Acknowledgements:** This study is supported by the Special Research Grant for the
529 Water Resources Industry (funding no. 201301070), the National Science Foundation
530 of China (funding no. 50479033), and the Basic Research Grant for Universities of
531 the Ministry of Education of China (funding no. 13lgjc01).

532



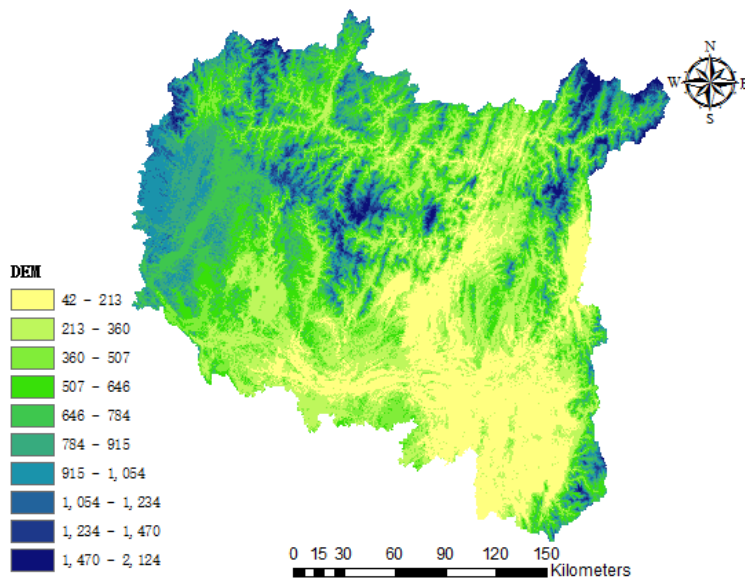
533 **Figures**



534

535

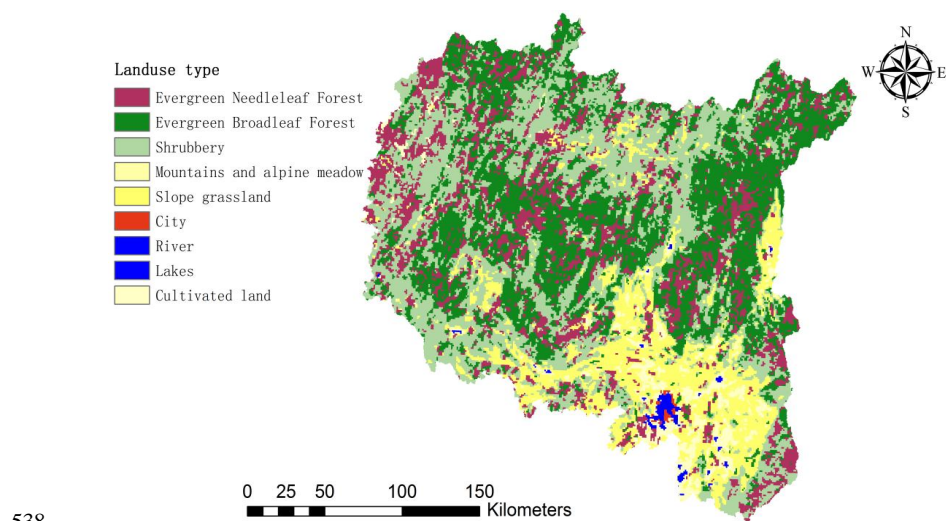
Fig. 1 sketch map of Liujiang River Basin



536

537

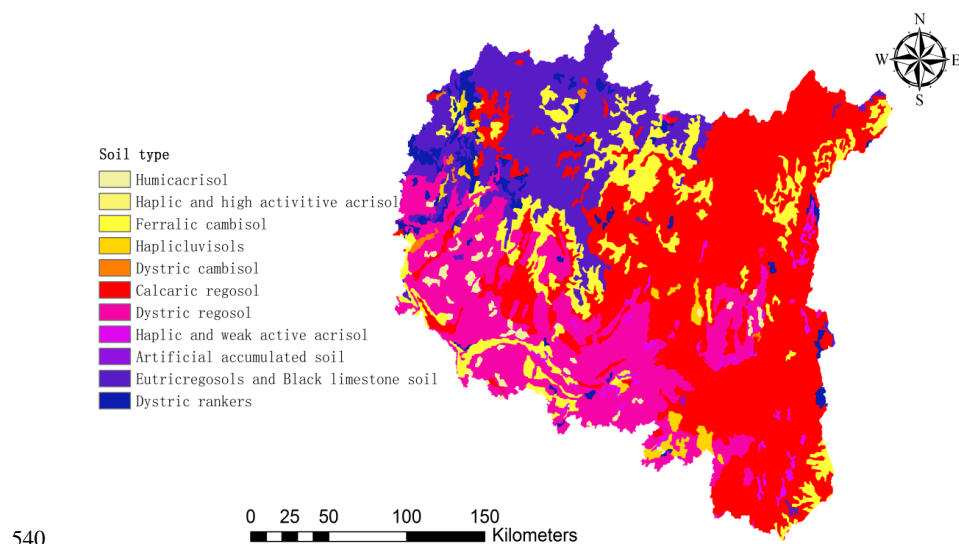
(a) DEM



538

539

(b) land use



540

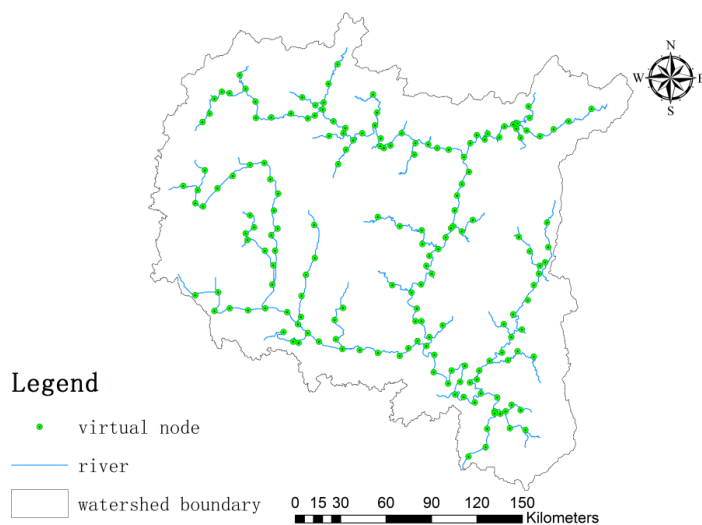
541

(c) soil type

542

Fig. 2 Terrain properties of LRB

543

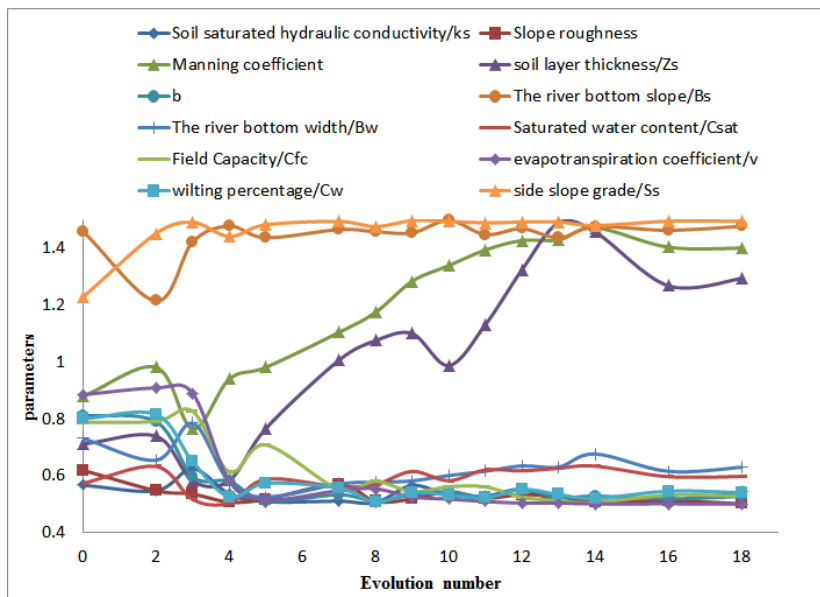


544

545

Fig. 3 Liuxihe Model structure set up for LRB (200m×200m resolution)

546



547

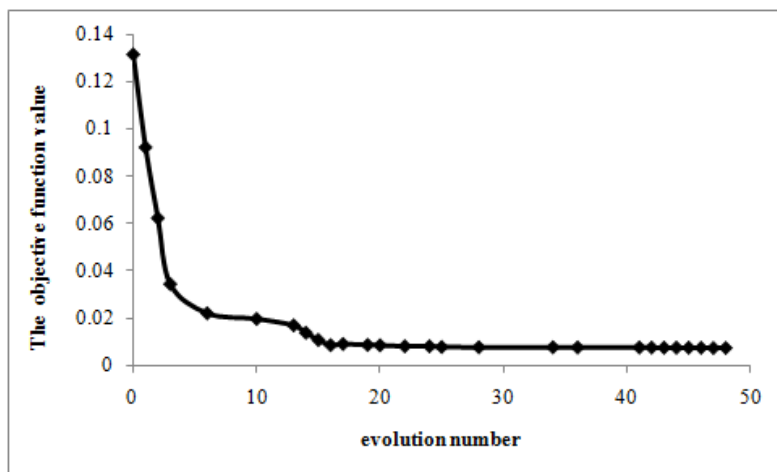
548

549

550

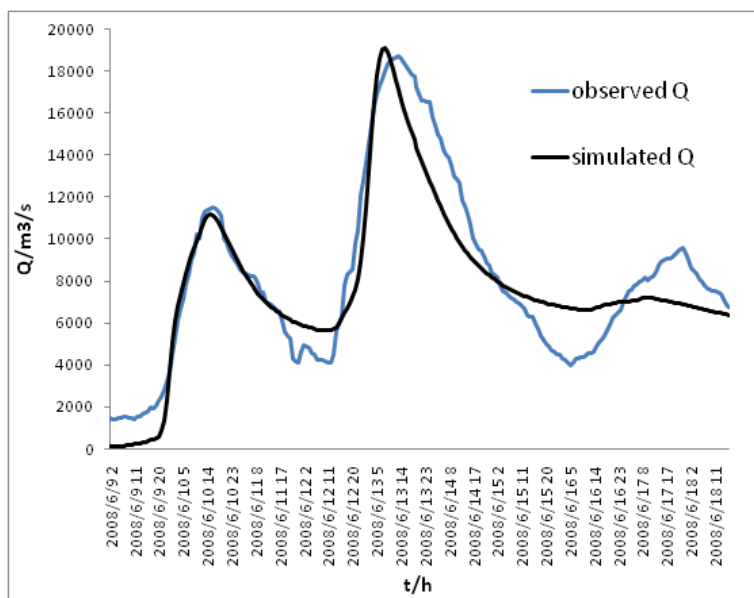
551

(a) Parameter evolution process



552
553
554
555

(b) Changing curve of objective function



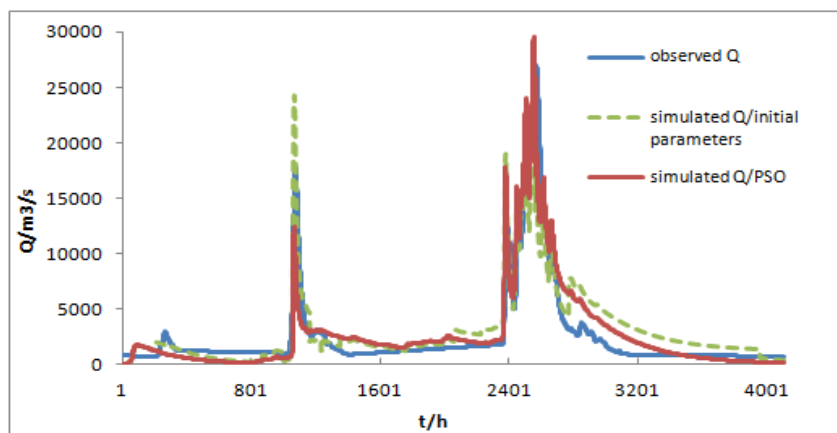
556
557
558
559

(c) Simulated flood process

Fig. 4 Parameter optimization results of Liuxihe Model for LRB with PSO algorithm

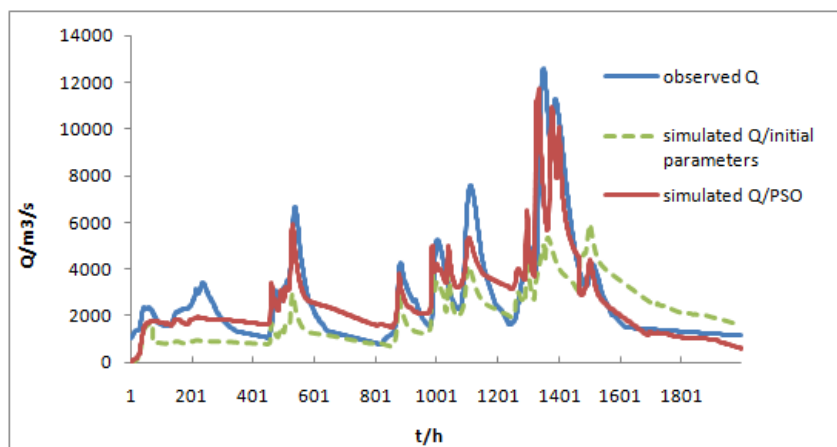


560
561



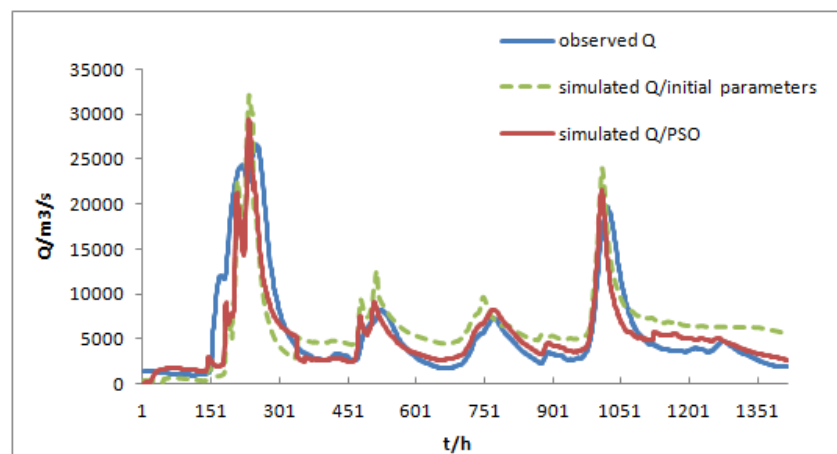
(a) flood event 1988051620

562
563

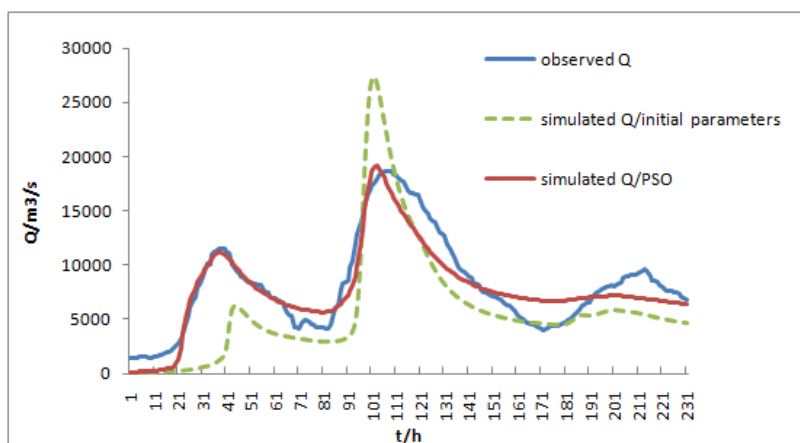


(b) flood event 1982042116

564
565



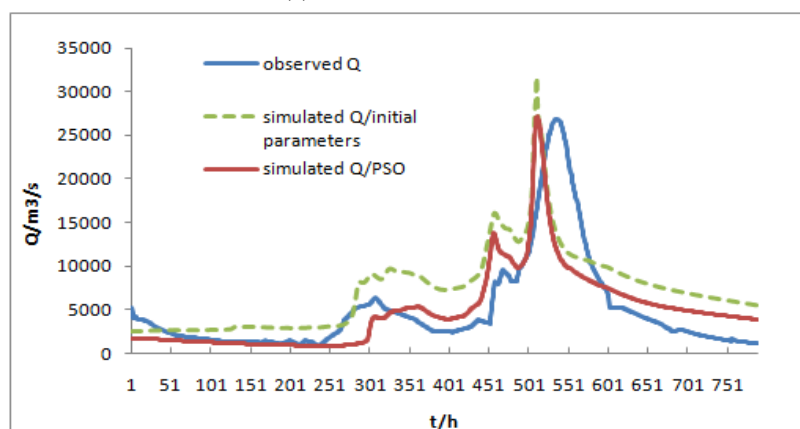
(c) flood event 1994060700



566

567

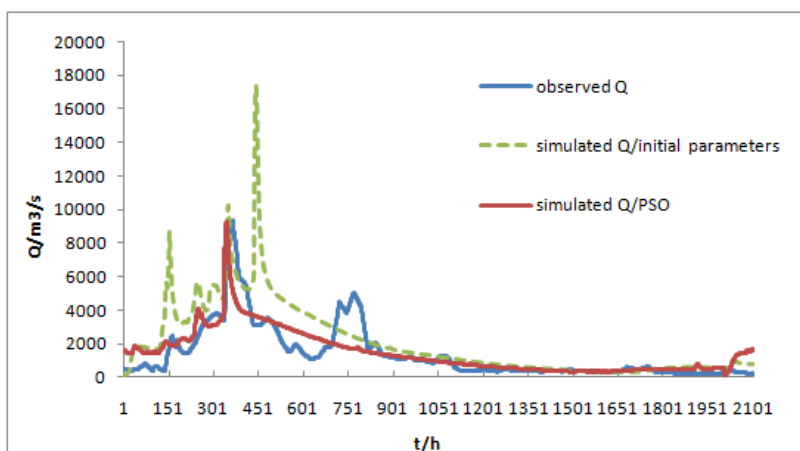
(d) flood event 2008060902



568

569

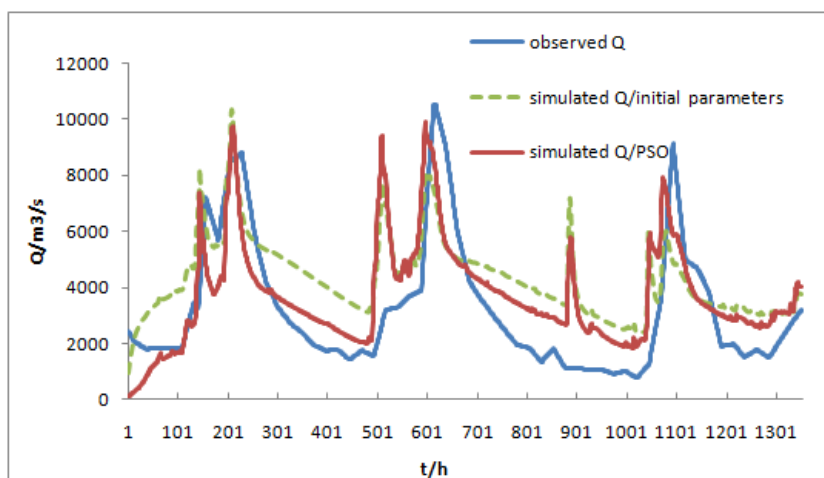
(e) flood event 200906090800



570

571

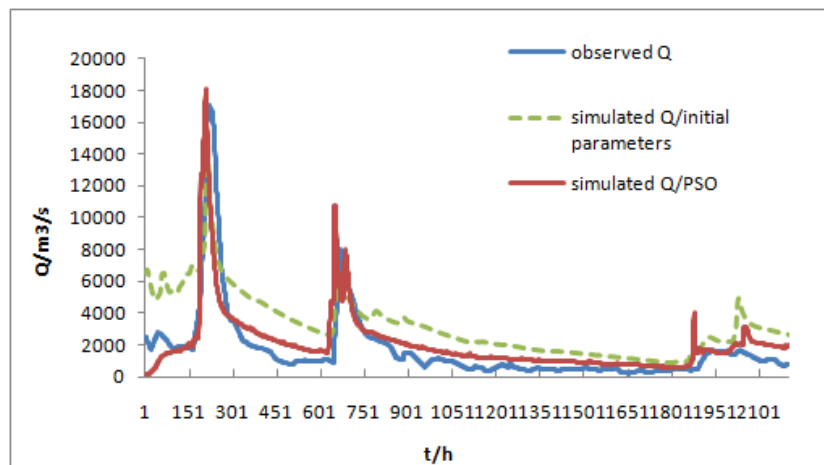
(f) flood event 201106010900



572

573

(g) flood event 201206022000



574

575

576

(h) flood event 201306011400

Fig. 5 Simulated flood events by Liuxihe Model with optimized parameters

577

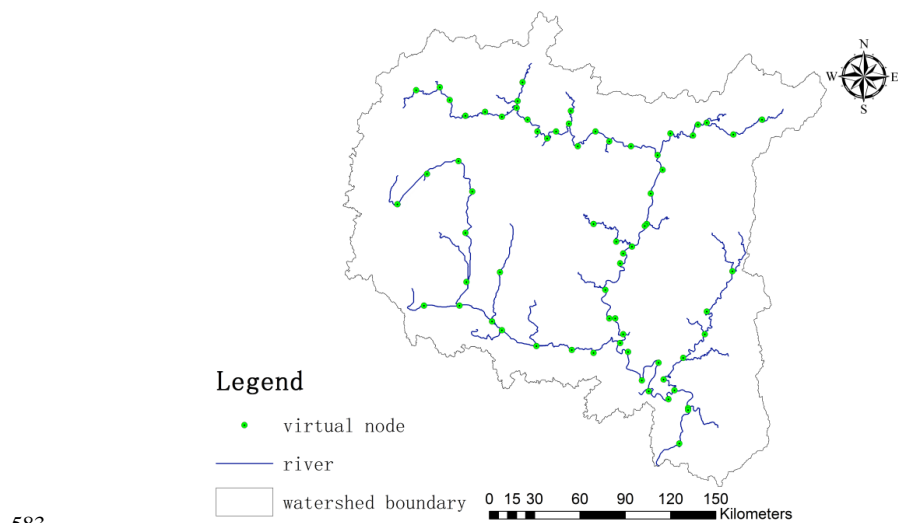
578

579

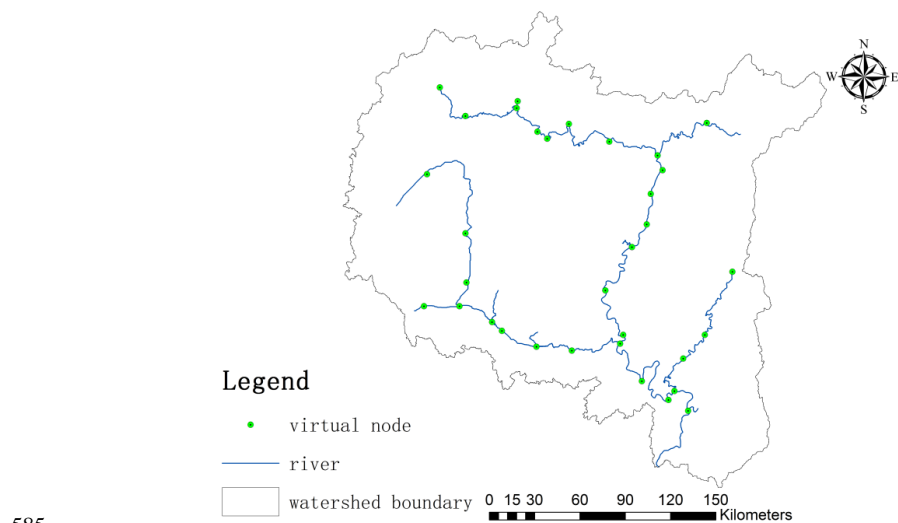
580

581

582



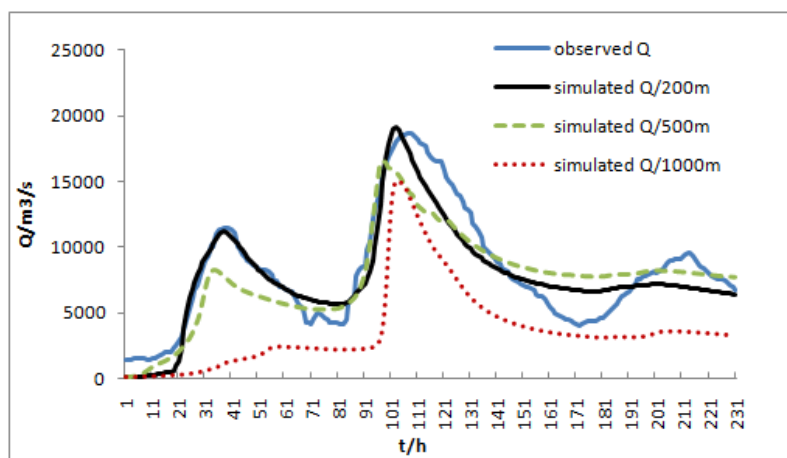
584 (a) 500m×500m resolution



586 (b) 1000m×1000m resolution

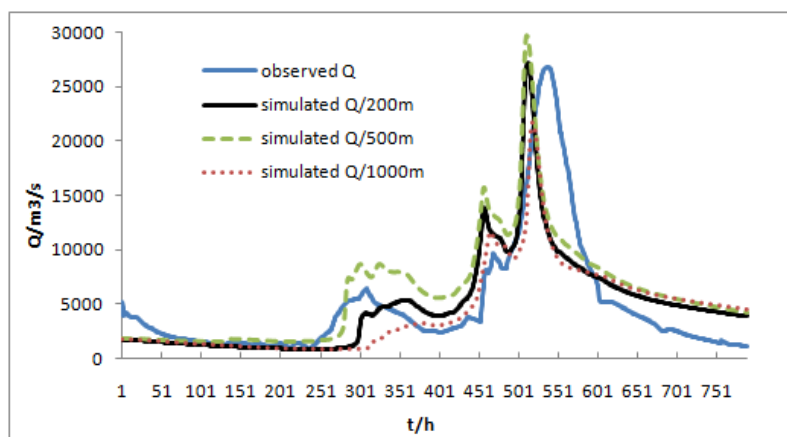
587 Fig. 6 Liuxihe Model structure set up for LRB with different resolution

588



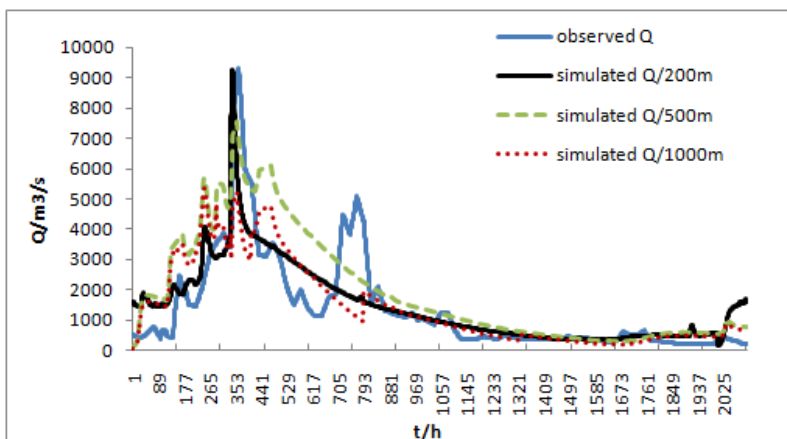
589
590

(a) flood event 2008060902



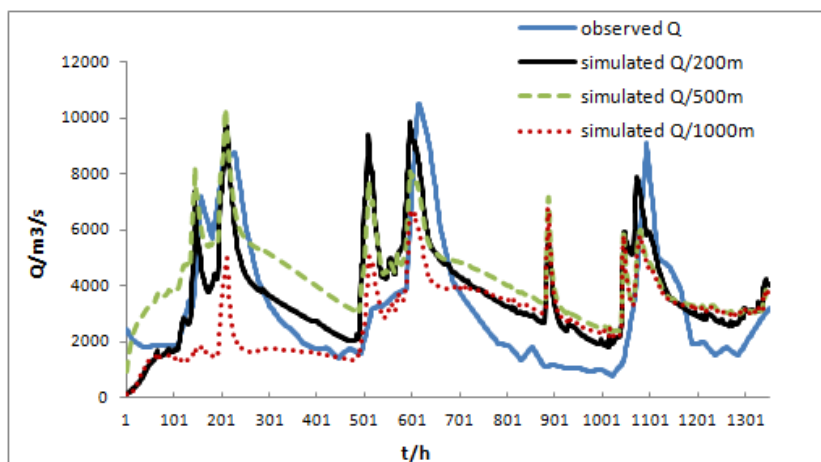
591
592

(b) flood event 2009060908



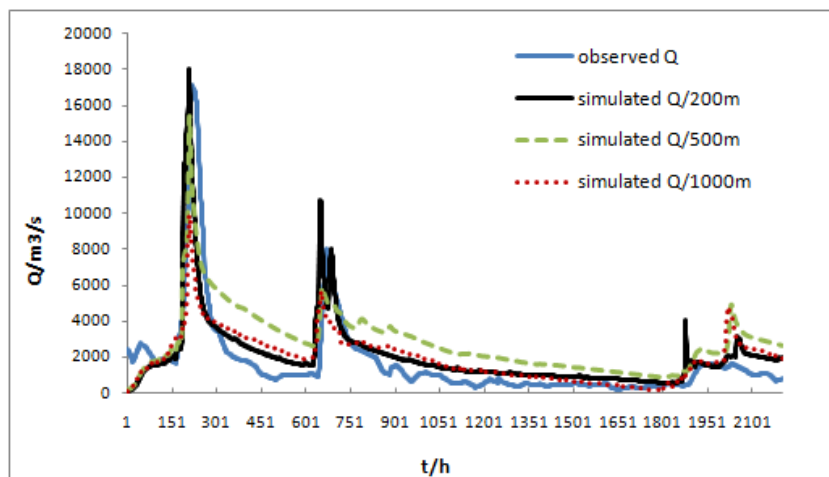
593
594

(c) flood event 2011060109



595
596

(d) flood event 2012060220



597
598

(e) flood event 2013060114

Fig. 7 Simulated results with different model resolutions

599
600
601
602
603
604
605

606 **Tables**

607

608

Table1 Brief information of flood events in LRB

<i>No.</i>	<i>Floods No.</i>	<i>Start time</i> (<i>yyyymmddhh</i>)	<i>End time</i> (<i>yyyymmddhh</i>)	<i>length of</i> <i>time/h</i>	<i>peak flow</i> (<i>m³/s</i>)
1	1982042116	1982042116	1982110216	4614	12600
2	1983020308	1983020308	1983021722	350	7880
3	1984021100	198402100	1984040105	1205	12900
4	1985011900	1985011900	1985021114	544	11400
5	1986022300	1986022300	1986042004	1334	12200
6	1987050100	1987050100	1987071700	1848	10800
7	1988070620	1988070620	1988100605	2915	27000
8	1989042600	1989042600	1989081009	2499	7500
9	1990050100	1990001000	1990072306	2006	11400
10	1991053118	1991053118	1991062806	686	14300
11	1992042900	1992042900	1992072107	1977	18100
12	1993060900	1993060900	1993082408	1818	21200
13	1994060700	1994060700	1994080706	1416	26500
14	1995052100	1995052100	1995071506	1296	17300
15	1996060600	1996060600	1996081808	1728	33700
16	1997060400	1997060400	1997062406	476	13600
17	1998051600	1998051600	1998090100	2520	19600
18	1990050100	1999050100	1999080404	1134	17800
19	2000052100	2000052100	2000061809	659	24100
20	2001051500	2001051500	2001062300	910	14200
21	2002042600	2002042600	2002081000	2520	17900
22	2003060600	2003060600	2003072103	843	11600
23	2004070300	200407000	2004081508	998	23700
24	2005061400	2005061400	2005070702	552	16400
25	2006060400	2006060400	2006071000	870	13200
26	2008060900	2008060900	2008061908	238	18700
27	2009060908	2009060908	2009071208	788	26800
28	2011061090	2011061009	2011090104	2004	9153
29	2012060220	2012060220	2012080101	1351	10500
30	2013060114	2013060114	2013090114	2200	17100

609

610

611

612



613
 614
 615

Table 2 The initial values of land use/cover related parameters

<i>Land use/cover</i>	<i>evaporation coefficient</i>	<i>roughness coefficient</i>
Evergreen needle leaf forest	0.7	0.4
Evergreen broadleaf forest	0.7	0.6
Shrubbery	0.7	0.4
Mountains and alpine meadow	0.7	0.2
Slope grassland	0.7	0.3
City	0.7	0.05
Cultivated land	0.7	0.35

616
 617
 618
 619
 620
 621
 622

Table 3 The initial values of soil related parameters

<i>Soil Type</i>	<i>soil thickness</i>	<i>water content at saturation condition</i>	<i>water content at field condition</i>	<i>hydraulic conductivity at saturation condition</i>
Humicacrisol	800	0.65	0.32	3.5
Haplic and high active acrisol	900	0.57	0.43	4.2
Ferralic cambisol	850	0.63	0.38	20.5
Haplicluvisols	980	0.46	0.15	2.6
Dystric cambisol	950	0.55	0.41	14
Calcaric regosol	1100	0.62	0.24	5.6
Dystric regosol	840	0.45	0.27	12.5
Haplic and weak active acrisol	1050	0.58	0.16	4.6
Artificial accumulated soil	1000	0.63	0.34	5.5
Eutricregosols and Black limestone	550	0.75	0.27	3.5
Dystric rankers	380	0.78	0.36	8

623
 624
 625
 626
 627
 628



629

Table 4 Evaluation indices of the simulated flood events

ID	floods	parameters	Nash–Sutcliffe coefficient/C	Correlation coefficient/R	Process relative error/P	Peak flow relative error/E	Water balance coefficient/W
1	1982081219	initial	0.52	0.48	0.56	0.58	0.52
		optimized	0.84	0.75	0.30	0.01	0.83
2	1983020308	initial	0.60	0.55	0.45	0.26	0.65
		optimized	0.82	0.84	0.21	0.04	0.89
3	1984010100	initial	0.62	0.71	0.38	0.32	0.75
		optimized	0.75	0.89	0.26	0.14	0.96
4	1985010100	initial	0.58	0.57	0.35	0.33	0.85
		optimized	0.73	0.87	0.17	0.01	1.05
5	1986010100	initial	0.65	0.62	0.38	0.25	0.62
		optimized	0.83	0.85	0.23	0.04	0.94
6	1987050100	initial	0.76	0.45	0.35	0.36	0.58
		optimized	0.93	0.76	0.10	0.05	1.01
7	19880516200	initial	0.54	0.58	0.26	0.42	0.82
		optimized	0.84	0.80	0.15	0.04	0.90
8	1989042600	initial	0.52	0.55	0.55	0.25	0.62
		optimized	0.64	0.74	0.39	0.02	0.88
9	1990050100	initial	0.55	0.64	0.42	0.23	0.55
		optimized	0.85	0.87	0.14	0.03	0.85
10	1991053118	initial	0.63	0.62	0.40	0.18	0.68
		optimized	0.80	0.76	0.25	0.04	0.95
11	1992042900	initial	0.48	0.59	0.35	0.34	0.65
		optimized	0.66	0.84	0.20	0.11	0.89
12	1993060900	initial	0.75	0.65	0.38	0.28	0.84
		optimized	0.91	0.89	0.24	0.09	1.05
13	1994060700	initial	0.78	0.64	0.32	0.26	1.25
		optimized	0.93	0.85	0.14	0.04	0.85
14	1995052100	initial	0.68	0.48	0.42	0.35	0.65
		optimized	0.82	0.70	0.20	0.01	0.81
15	1996060600	initial	0.74	0.65	0.25	0.23	0.54
		optimized	0.90	0.93	0.18	0.02	0.86
16	1997060400	initial	0.65	0.51	0.23	0.26	0.65
		optimized	0.84	0.87	0.13	0.06	0.95
17	1998051600	initial	0.57	0.62	0.35	0.18	0.68
		optimized	0.83	0.85	0.30	0.01	1.05
18	1999061700	initial	0.48	0.59	0.33	0.15	0.55
		optimized	0.60	0.83	0.15	0.05	0.80
19	2000052100	initial	0.67	0.62	0.45	0.25	0.58
		optimized	0.79	0.89	0.26	0.06	0.83
20	2001051500	initial	0.62	0.56	0.32	0.22	0.68



		optimized	0.80	0.82	0.25	0.07	0.82
21	2002042600	initial	0.68	0.65	0.38	0.18	0.57
		optimized	0.86	0.90	0.24	0.02	0.87
22	2003060600	initial	0.75	0.55	0.25	0.26	0.55
		optimized	0.92	0.85	0.14	0.04	0.76
23	2004070300	initial	0.58	0.68	0.38	0.27	0.68
		optimized	0.78	0.82	0.23	0.08	0.85
24	2005061400	initial	0.65	0.62	0.52	0.32	0.65
		optimized	0.76	0.76	0.35	0.06	0.74
25	2006060400	initial	0.68	0.72	0.62	0.35	0.53
		optimized	0.82	0.83	0.30	0.10	0.86
26	2009060908	initial	0.75	0.78	0.25	0.23	1.22
		optimized	0.95	0.92	0.17	0.04	0.09
27	2011010100	initial	0.66	0.75	0.35	0.55	1.66
		optimized	0.80	0.84	0.26	0.03	1.02
28	2012010100	initial	0.63	0.68	0.34	0.22	1.42
		optimized	0.82	0.79	0.20	0.05	0.80
29	2013010100	initial	0.78	0.65	0.31	0.32	1.35
		optimized	0.95	0.82	0.20	0.06	0.92
	average	initial	0.64	0.62	0.37	0.29	0.78
		optimized	0.82	0.83	0.22	0.05	0.87

630

631

632

633 Table 5 Grid cell numbers with different model spatial resolution

<i>model resolution</i>	<i>Number of grid cells</i>	<i>Number of hill slope cells</i>	<i>Number of river cells</i>
200m*200m	1469900	1463204	6696
500m*500m	235184	234113	1071
1000m*1000m	58796	58528	268

634

635

636

637



638 Table 6 Optimized parameters with different model spatial resolution

Resoluti on	Soil saturated hydraulic conductivit y/ks	Slope roughnes s	Manning coefficien t	Soil layer thickness/Zs	b	The river bottom slope/Bs
	1.33	0.66	1.19	1.42	0.67	0.75
200m	The river bottom width/Bw	Saturated water content/C sat	Field Capacity/ Cfc	Evapotranspir ation coefficient/v	Wilting percentage/ Cw	Side slope grad e/Ss
	1.24	1.11	1.2	0.94	0.68	1.42
500m	Soil saturated hydraulic conductivit y/ks	Slope roughnes s	Manning coefficien t	Soil layer thickness/Zs	b	The river bottom slope/Bs
	0.67	1.47	1.49	1.37	1.5	0.51
1000m	The river bottom width/Bw	Saturated water content/C sat	Field Capacity/ Cfc	Evapotranspir ation coefficient/v	Wilting percentage/ Cw	Side slope grad e/Ss
	0.91	1.16	1.41	1.37	1.37	0.5
1000m	Soil saturated hydraulic conductivit y/ks	Slope roughnes s	Manning coefficien t	Soil layer thickness/Zs	b	The river bottom slope/Bs
	0.5	1.43	1.17	1.11	1.47	0.57
1000m	The river bottom width/Bw	Saturated water content/C sat	Field Capacity/ Cfc	Evapotranspir ation coefficient/v	Wilting percentage/ Cw	Side slope grad e/Ss
	1.1	0.76	0.53	0.6	1.5	0.54

639

640

641 **References**

- 642 [1] Abbott, M.B. et al.: An Introduction to the European Hydrologic System-System Hydrologue Europeen,
643 'SHE', a: History and Philosophy of a Physically-based, Distributed Modelling System, Journal of
644 Hydrology, 87, 45-59, 1986.
- 645 [2] Abbott, M.B. et al.: An Introduction to the European Hydrologic System-System Hydrologue Europeen,
646 'SHE', b: Structure of a Physically based, distributed modeling System, Journal of Hydrology, 87, 61-77,
647 1986.
- 648 [3] Ambrose, B., Beven, K., and Freer, J.: Toward a generalization of the TOPMODEL concepts: Topographic
649 indices of hydrologic similarity, Water Resour. Res., 32, 2135-2145, 1996.
- 650 [4] Anderson, A. N., McBratney, A. B., and FitzPatrick, K. E. A soil mass, surface and spectral fractal dimensions
651 estimated from thin section photographs. Soil Sci. Soc. Am. J., 60, 962-969, 1996.
- 652 [5] Arya, L.M., and J.F. Paris. 1981. A physioempirical model to predict the soil moisture characteristic from
653 particle-size distribution and bulk density data. Soil Sci. Soc. Am. J. 45, 1023-1030.
- 654 [6] Bartholmes, J.C., Thielen, J., Ramos, M.H., Gentilini, S., 2009. The european flood alert system EFAS e part
655 2: statistical skill assessment of probabilistic and deterministic operational forecasts. Hydrol. Earth Syst. Sci.
656 13 (2), 141e153.
- 657 [7] Burnash, R. J. C., 1995. "The NWS river forecast system-catchment modeling." Computer models of
658 watershed hydrology, V. P. Singh, ed., Water Resource Publications, Littleton, Colo., 311-366.
- 659 [8] Catto  n, C  dine, Hilary McMillan, and Stuart Moore. Coupling a high-resolution weather model with a
660 hydrological model for flood forecasting in New Zealand[J]. Journal of Hydrology (NZ), 2016,55 (1): 1-23.
- 661 [9] Chen, Xiuwan, Analysis on flood disasters in China, 1995. Marine Geology and Quaternary Geology,
662 15(3):161-168.
- 663 [10] Chen, Huiquan, Mao Shimin. Calculation and Verification of an Universal Water Surface Evaporation
664 Coefficient Formula[J]. Advances in Water Science, 1995, 6(2):116-120.
- 665 [11] Chen, Yangbo. Liuxihe Model, China Science and Technology Press, September 2009.
- 666 [12] Chen, Yangbo, Ren, Q.W., Huang, F.H., Xu, H.J., and Cluckie, I.: Liuxihe Model and its modeling to river
667 basin flood, Journal of Hydrologic Engineering, 16,33-50, 2011.
- 668 [13] Chen, Yangbo, Yi Dong, Pengcheng Zhang. Study on the method of flood forecasting of small and medium
669 sized catchment, proceeding of the 2013 annual meeting of the Chinese Society of Hydraulic Engineering,
670 1001-1008, 2013.
- 671 [14] Chen, Yangbo, Ji Li, Huijun Xu. Improving flood forecasting capability of physically based distributed
672 hydrological model by parameter optimization. Hydrology & Earth System Sciences, 20,375-392, 2016.
- 673 [15] Dibike, Y. B., P. Coulibaly. Hydrologic impact of climate change in the Saguenay watershed: comparison of
674 downscaling methods and hydrologic models[J]. Journal of Hydrology, 2005, 307(1-4): 145-163.
- 675 [16] EEA, 2010. Mapping the Impacts of Natural Hazards and Technological Accidents in Europe: an Overview
676 of the Last Decade. EEA Technical Report. European Environment Agency, Copenhagen, p. 144.
- 677 [17] Falorni, G., Teles, V., Vivoni, E. R., Bras, R. L., and Amaratunga, K. S.: Analysis and characterization of the
678 vertical accuracy of digital elevation models from the Shuttle Radar Topography Mission, J. Geophys. Res.
679 F-Earth Surf., 110, F02005, doi:10.1029/2003JF000113, 2005.
- 680 [18] Freeze, R. A., and Harlan, R.L.: Blueprint for a physically-based, digitally simulated, hydrologic response
681 model, Journal of Hydrology, 9,237-258,1969.
- 682 [19] Grayson, R.B., Moore, I. D., and McMahon, T.A.: Physically based hydrologic modeling: I. A Terrain-based
683 model for investigative purposes, Water Resources Research, 28,2639-2658,1992.
- 684 [20] Guo, Hanqing, Hua Youzhi, Bai Xiumei. Hydrological Effects of Litter on Different Forest Stands and Study
685 about Surface Roughness Coefficient[J]. Journal of Soil and Water Conservation, 2010, 24(2):179-183
- 686 [21] Jensen, S. K. and J. O. dominggue, 1988, Extracting Topographic Structure from Digital Elevation Data for
687 Geographic Information System Analysis, Photogrammetric Engineering and Remote Sensing, 54(11)
- 688 [22] Jia, Y., Ni, G., and Kawahara, Y.: Development of WEP model and its application to an urban watershed,
689 Hydrological Processes, 15,2175- 2194,2001.
- 690 [23] Julien, P.Y., Saghafian, B., and Ogden, F. L.: Raster-Based Hydrologic Modeling of spatially-Variied Surface
691 Runoff, Water Resources Bulletin, 31,523-536,1995.
- 692 [24] Kauffeldt, A., F. Wetterhall, F. Pappenberger, P. Salamon, J. Thielen. Technical review of large-scale
693 hydrological models for implementation in operational flood forecasting schemes on continental level[J].
694 Environmental Modelling & Software, 2016, 75: 68-76.
- 695 [25] Kavvas, M., Chen, Z., Dogrul, C., Yoon, J., Ohara, N., Liang, L., Aksoy, H., Anderson, M., Yoshitani, J.,
696 Fukami, K., and Matsuura, T. (2004). "Watershed Environmental Hydrology (WEHY) Model Based on
697 Upscaled Conservation Equations: Hydrologic Module." J. Hydrol. Eng.,
698 10.1061/(ASCE)1084-0699(2004)9:6(450), 450-464.
- 699 [26] Kouwen, N.: WATFLOOD: A Micro-Computer based Flood Forecasting System based on Real-Time
700 Weather Radar, Canadian Water Resources Journal, 13,62-77,1988.
- 701 [27] Krzmm, R. W. The Federal Role in Natural Disasters. International Symposium on Torrential Rain and
702 Flood, Oct 5-9, 1992, Huangshan, China.
- 703 [28] Kuniyoshi, T. Japanese Experiences of Combating Against Floods in the past half century. International
704 Symposium on Torrential Rain and Flood, Oct 5-9, 1992, Huangshan, China.



- 705 [29] Li, Y., C. Wang. Impacts of urbanization on surface runoff of the Dardenne Creek watershed, St. Charles
706 County, Missouri[J]. Phys. Geogr. 2009, 30(6):556-573.
- 707 [30] Li, Yuting, Zhang Jianjun, Ri Hao, et al. Effect of Different Land Use Types on Soil Anti-scourability and
708 Roughness in Loess Area of Western Shanxi Province[J]. Journal of Soil and Water Conservation, 2013,
709 27(4):1-6.
- 710 [31] Liang, X., Lettenmaier, D.P., Wood, E.F., and Burges, S.J.:A simple hydrologically based model of land
711 surface water and energy fluxes for general circulation models, J. Geophys. Res, 99,14415-14428,1994.
- 712 [32] Liao, Zhenghong, Yangbo Chen, Xu Huijun, Yan Wanling, Ren Qiwei, Parameter Sensitivity Analysis of the
713 Liuxihe Model Based on E-FAST Algorithm, Tropical Geography, 2012, 32(6):606-612.
- 714 [33] Liao, Zhenghong, Yangbo Chen, Xu Huijun, He Jinxiang, Study of Liuxihe Model for flood forecast of
715 Tiantoushui Watershed, Yangtze River, 2012, 43(20): 12-16.
- 716 [34] Lohmann, D., Raschke, E., Nijssen, B., Lettenmaier, D. P. (1998). Regional scale hydrology: II. Application
717 of the VIC-2L model to the Weser River, Germany, Hydrological Sciences Journal, 43:1, 143-158.
- 718 [35] Loveland, T. R., Merchant, J. W., Ohlen, D. O., and Brown, J. F.:Development of a Land Cover
719 Characteristics Data Base for the Conterminous U.S., Photogram. Eng. Remote Sens., 57, 1453-1463, 1991.
- 720 [36] Loveland, T. R., Reed, B. C., Brown, J. F., Ohlen, D. O., Zhu, J., Yang, L., and Merchant, J. W.:
721 Development of a Global Land Cover Characteristics Database and IGBP DISCover from 1-km AVHRR
722 Data, Int. J. Remote Sens., 21, 1303-1330, 2000.
- 723 [37] Madsen, H.:Parameter estimation in distributed hydrological catchment modelling using automatic
724 calibration with multiple objectives, Advances in Water Resources, 26,205-216, 2003.
- 725 [38] Olivera, F., B. B. DeFee. Urbanization and its effect on runoff in the Whiteoak Bayou Watershed, Texas[J]. J.
726 Am. Water Resour. Assoc. , 2007, 43(1):170-182.
- 727 [39] Ott, B., Uhlenbrook S. Quantifying the impact of land-use changes at the event and seasonal time scale using
728 a process-oriented catchment model[J]. Hydrol Earth Syst Sci. ,2004, 8:62-78.
- 729 [40] Refsgaard, J. C.,1997. "Parameterisation, calibration and validation of distributed hydrological models." J.
730 Hydrol., 198, 69-97.
- 731 [41] Rose, Seth Norman E. Peters. Effects of urbanization on streamflow in the Atlanta area (Georgia, USA): a
732 comparative hydrological Approach[J]. Hydrological Processes, 2001, 15(8):1141-1157.
- 733 [42] Rwetabula, J., F. De Smedt, M. Rebhun. Prediction of runoff and discharge in the Simiyu River (tributary of
734 Lake Victoria, Tanzania) using the WetSpa model. Hydrology and Earth System Sciences Discussions,
735 European Geosciences Union, 2007, 4 (2):881-908.
- 736 [43] Shafii, M. and Smedt, F. De: Multi-objective calibration of a distributed hydrological model (WetSpa) using
737 a genetic algorithm, Hydrol. Earth Syst. Sci., 13, 2137-2149, 2009.
- 738 [44] Sharma, A. Tiwari, K. N.: A comparative appraisal of hydrological behavior of SRTM DEM at catchment
739 level, J. Hydrol., 519, 1394-1404, 2014.
- 740 [45] Shen, Shengqiong, Shuanghe, Guze. Conversion Coefficient between Small Evaporation Pan and
741 Theoretically Calculated Water Surface Evaporation in China[J].Journal of Nanjing Institute of Meteorology,
742 2007, 30(4):561-565.
- 743 [46] Sood, A., Smakhtin, V., 2015. Global hydrological models: a review. Hydrol. Sci. J. 60(4), 549e565.
744 <http://dx.doi.org/10.1080/02626667.2014.950580>.
- 745 [47] Stisen, Simon, Jensen, Karsten H., Inge Sandholt , David I.F. Grimes. A remote sensing driven distributed
746 hydrological model of the Senegal River basin, Journal of Hydrology, 2008(354):131-148.
- 747 [48] Strahler, A. N.Quantitative analysis of watershed Geomorphology, Transactions of the American Geophysical
748 Union, 1957, 35(6), 913-920.
- 749 [49] Sugawara, M. _1995_. "Tank model." Computer models of watershed hydrology, V. P. Singh, ed., Water
750 Resources Publications, Littleton, Colo., 165-214.
- 751 [50] Thielen, J., Bartholmes, J., Ramos, M.H., de Roo, A., 2009. The European flood alert system e part 1:
752 concept and development. Hydrol. Earth Syst. Sci. 13 (2), 125-140.
- 753 [51] Thielen, J., Pappenberger, F., Salamon, P., Bogner, K., Burek, P., de Roo, A., 2010. The State of the Art of
754 Flood Forecasting-Hydrological Ensemble Prediction Systems, p. 145.
- 755 [52] Todini, E., 1996. "The ARNO rainfall-runoff model." J. Hydrol., 175, 339-382.
- 756 [53] Vanrheenen, N. T., A W Wood, R N Palmer, et al. Potential implications of PCM climate change scenarios for
757 Sacramento-San Joaquin River Basin hydrology and water resources[J]. Climatic Change, 2004, 62(1-3):
758 257-281.
- 759 [54] Vieux, B. E., and Vieux, J. E.:VfloTM: A Real-time Distributed Hydrologic Model[A]. In:Proceedings of the
760 2nd Federal Interagency Hydrologic Modeling Conference, July 28-August 1, Las Vegas, Nevada. Abstract
761 and paper on CD-ROM, 2002.
- 762 [55] Vieux, B.E., Moreda, F.G.:Ordered physics-based parameter adjustment of a distributed model. In: Duan, Q.,
763 Sorooshian, S., Gupta, H.V., Rousseau, A.N., Turcotte, R. (Eds.), Advances in Calibration of Watershed
764 Models. Water Science and Application Series, vol. 6. American Geophysical Union, pp. 267-281, 2003
- 765 [56] Vieux, B.E., Cui Z., Gaur A.: Evaluation of a physics-based distributed hydrologic model for flood
766 forecasting, Journal of Hydrology, 298, 155-177, 2004.
- 767 [57] Vivoni, E.R., Ivanov, V.Y., Bras, R.L. and Entekhabi, D. 2004. Generation of Triangulated Irregular
768 Networks based on Hydrological Similarity. Journal of Hydrologic Engineering. 9(4): 288-302.
- 769 [58] Wang, Z., Batelaan, O., De Smedt, F.: A distributed model for water and energy transfer between soil, plants
770 and atmosphere (WetSpa). Journal of Physics and Chemistry of the Earth 21, 189-193, 1997.



- 771 [59] Wigmosta, M. S., Vai, L. W., and Lettenmaier, D. P.: A Distributed Hydrology-Vegetation Model for
772 Complex Terrain, *Water Resources Research*, 30,1665-1669,1994.
- 773 [60] Witold F. Krajewski, Daniel Ceynar, Ibrahim Demir, Radoslaw Goska, Anton Kruger, Carmen Langel,
774 Ricardo Mantilla, James Niemeier, Felipe Quintero, Bong-Chul Seo, Scott J. Small, Larry J. Weber, and
775 Nathan C. Young. Real-time Flood Forecasting and Information System for the State of Iowa[J] *Bull.*
776 *Amer.Meteor.* 2016,Soc. doi:10.1175/BAMS-D-15-00243.1, in press.
- 777 [61] Xu, Huijuna, Yangbo Chen, Zeng Biqu, He Jinxiang, Liao Zhenghong, Application of SCE-UA Algorithm
778 to Parameter Optimization of Liuxihe Model, *Tropical Geography*, 2012.1, 32(1): 32-37.
- 779 [62] Xu, Huijun, Yangbo Chen, Li Zhouyang, He Jinxiang, Analysis on parameter sensitivity of distributed
780 hydrological model based on LH-OAT Method, *Yangtze River*, 2012, 43(7): 19-23.
- 781 [63] Yang, D., Herath ,S. and Musiaka, K.:Development of a geomorphologic properties extracted from DEMs
782 for hydrologic modeling, *Annual journal of Hydraulic Engineering, JSCE*, 47,49-65,1997.
- 783 [64] Zaradny, H. *Groundwater Flow in Saturated and Unsaturated Soil*. Now York:A A BalKema,1993.
- 784 [65] Zhang, Shaohui, Xu Di, Li Yinong, et al. An optimized inverse model used to estimate Kostikov infiltration
785 parameters and Manning's roughness coefficient based on SGA and SRFR model: I Establishment[J]. *Shuili*
786 *Xuebao*, 2006, 37(11):1297-1302.
- 787 [66] Zhang, Shaohui, Xu Di, Li Yinong, et al. Optimized inverse model used to estimate Kostikov infiltration
788 parameters and Manning's roughness coefficient based on SGA and SRFR model: II Application[J]. *Shuili*
789 *Xuebao*, 2007, 38(4):402-408.
- 790 [67] Zhang, Mengze, Liu Yuanhong, Wang Lingru, et al. Inversion on Channel Roughness for Hydrodynamic
791 Model by Using Quantum-Behaved Particle Swarm Optimization[J]. *Yellow River*, 2015, 37(2):26-29
- 792 [68] Zhao, R. J.,1977. Flood forecasting method for humid regions of China, East China College of Hydraulic
793 Engineering, Nanjing, China.